

PREPARATION OF 2-DEOXY-D-GLUCOSE COATED SPIO NANOPARTICLES AND CHARACTERIZATION OF THEIR PHYSICAL, CHEMICAL, AND BIOLOGICAL PROPERTIES

A. M. MAHARRAMOV, M. A. RAMAZANOV*, A. I. AHADOVA^a,
M. KLOOR^a, JUERGEN KOPITZ^a, M. VON KNEBEL DOEBERITZ^a,
A. L. SHABANOV, Q.M. EYVAZOVA, Z.A.AGAMALIYEV, F.V.HAJIYEVA,
S.B.VELIYEVA, U. A. HASANOVA

Baku State University, Nano Research Laboratory, Azerbaijan Baku, Zahid Khalilov Str.23

^aUniversity of Heidelberg, Department of Applied Tumor Biology, Institute of Pathology, Im Neuenheimer Feld 224, 69120 Heidelberg, Germany

A new water-dispersible nanostructure based superparamagnetic iron oxide nanoparticles (SPIONs)(Fe₃O₄) coated by 2-Deoxy-D-Glucose (2DG) was prepared in a well-shaped spherical form using the method of chemical co-precipitation. Scanning Electron Microscopy (SEM) and Atomic Force Microscopy (AFM) methods demonstrated that the prepared nanoparticles (NPs) were well individualized and homogeneous in size. Quantitative analysis of coupled 2DG was performed by atom absorbance spectroscopy. The samples also were analyzed by Fourier Transform Infrared (FTIR) and X-ray diffraction spectroscopy. Biological activity of the prepared nanostructures was proven by growth inhibition of colorectal cancer cell lines.

(Received September 29, 2014; Accepted November 7, 2014)

Keywords: Nanoparticles, Glucose, SPION, drug delivery

1. Introduction

In recent years great attention has been paid to the application of nanotechnological approaches in different areas of science. The idea of modifying compounds with known properties in bulk state by passing them into nanoscale is especially attractive, because certain compounds in nanoscale can show new and unexpected features [1]. In particular, the preparation and characterization of nanomaterials for biomedical application have been of great scientific and technological interest. Magnetite nanoparticles (NPs) are very interesting and promising for biomedical application due to their biocompatibility and low toxicity in the human body [2]. Consequently, the potential application of SPIONs includes high-density cellular therapy, tissue repair, magnetic resonance imaging (MRI), hyperthermia, and magnetofection [3,4]. In particular, nanoparticles have become attractive because of their ability to deliver drugs specifically to the site of interest. This allows to enhance the concentration of the drug in certain tissues and to reduce the damage to surrounding tissues by site-directed application.

The synthesis of NPs is connected with surface stabilization of forming NPs, in order to prevent their further agglomeration. Many different biocompatible molecules, which can stabilize and functionalize the surface of NPs [5] have been suggested for biomedical application: biodegradable polymers [6], phospholipids [7,8], surfactants, biological polymers (polynucleotides [9-13], carbohydrates [14,15], proteins [16,17], peptides [18,19]) and etc. [20-25]

In the present study, we focused on 2DG as a molecule to be coupled to NPs. 2DG is a synthetic analogue of glucose in which the hydroxyl group bound to the second carbon is replaced

* Corresponding author: nanomaterials@bsu.az

by a hydrogen atom. Since the discovery of aerobic glycolysis by Otto Warburg it is known that cancer cells, independently from oxygen supply, predominantly rely on the glycolytic pathway of glucose metabolism and energy synthesis despite low energy gain in comparison to oxidative phosphorylation. This discovery led to idea of novel cancer treatment method by blocking glycolytic pathway in cancer cells using the glucose analogue 2DG [26]. However, the application of 2DG in the clinical setting is limited due to possible toxicity [27].

Coupling 2DG to NPs may help to overcome toxicity and therefore represent a promising approach for future anti-cancer treatment approaches and various other potential applications in the biomedical field.

In the present paper we report a simple, one-pot preparation of water-dispersible Fe_3O_4 nanoparticles coupled with 2-Deoxy-D-Glucose (2DG) using the method of chemical wet co-precipitation without any surfactant application.

2. Materials and methods

Materials

All chemicals were used as received. $\text{FeCl}_3 \cdot 6\text{H}_2\text{O}$, $\text{FeSO}_4 \cdot 7\text{H}_2\text{O}$, NH_4OH (25 %), 2DG was purchased from Sigma-Aldrich (Taufkirchen, Germany).

Synthesis of Fe_3O_4 coated by 2DG NPs

Magnetic iron oxide nanoparticles are usually prepared by wet chemical precipitation from aqueous iron salt solutions in alkaline milieu created by using NH_4OH or NaOH [35]. Fe_3O_4 coated by 2DG NPs were synthesized by chemical co-precipitation of $\text{FeCl}_3 \cdot 6\text{H}_2\text{O}$ and $\text{FeSO}_4 \cdot 7\text{H}_2\text{O}$ with subsequent stabilization with 2DG. Briefly, $\text{FeCl}_3 \cdot 6\text{H}_2\text{O}$ (0.01 M) and $\text{FeSO}_4 \cdot 7\text{H}_2\text{O}$ (0.006 M) were dissolved in 200 mL of deionized water under the bubbling of gaseous N_2 . Then, 25% aqueous ammonia solution (1.5 M) containing 2DG (in excess) was dropped into solution with vigorous stirring until the pH of the solution raised to 9.5. The formed magnetite coated by 2DG after reaction was separated with strong NdFeB permanent magnet and repeatedly washed with distilled water. Then the obtained nanoparticles were dried at ambient conditions and the iron content in the sample was analyzed by atom absorption spectroscopy and performed on Varian SpectrAA 220FS Atomic absorption spectrometer. Samples were prepared by Milestone ETHOS 1 Microwave extraction unit.

Characterization of nanostructure

FT-IR

The functional groups present in the powder samples of $\text{Fe}_3\text{O}_4@2\text{DG}$ NPs were identified by Fourier Transform Infrared (FTIR) spectroscopy. FTIR spectra were recorded on a Varian 3600 FTIR spectrophotometer in KBr tablets. The spectrum was taken in the range of 4000-400 cm^{-1} at room temperature.

XRD

X-ray diffraction (XRD) analysis was performed on Rigaku Mini Flex 600 XRD diffractometer at room temperature. In all cases, $\text{Cu K } \alpha$ radiation from a Cu X-ray tube (run at 15 mA and 30 kV) was used. The samples were scanned in the Bragg angle 2θ range of 10–70°. The purity and crystalline properties of the $\text{Fe}_3\text{O}_4@2\text{DG}$ were investigated by powder XRD.

Scanning Electron Microscope (SEM) and Energy-Dispersive Spectrum (EDS) analysis

SEM and EDS analysis of prepared samples of $\text{Fe}_3\text{O}_4@2\text{DG}$ composite nanoparticles were taken on Field Emission Scanning Electron Microscope JEOLJSM-7600F at an accelerating

voltage of 10 kV, SEI regime.

AFM analysis

The morphology of samples was studied by means of AFM Integra-Prima (NT-MDT, Russia). Special silica cantilevers, covered by ferromagnetics with curvature radii of 20 nm and a resonance frequency of 40-97 Hz were used for the scanning. The scanning area was 500×500 nm. The measurements were implemented in semi-contact regime on air, and the determination of changes of cantilever amplitude oscillation allowed definition of the surface topography. Scanning rate was 1.969 Hz and the number of scanned lines was 256.

MTS assay

Colorectal cancer cells (HCT116, HT29, RKO) were seeded in 96-well plates at a density of 104 cells per well in DMEM (Roswell Park Memorial Institute, Gibco, Paisley, UK) cell culture medium supplemented with 10% fetal bovine serum and 1% penicillin/streptomycin (Gibco, NY, USA). 2DG or 2DG-coupled nanoparticles ($\text{Fe}_3\text{O}_4@2\text{DG}$) were added to the wells at a concentration of 4 mM 2DG. 2DG concentration for $\text{Fe}_3\text{O}_4@2\text{DG}$ was determined by atom adsorption analysis. After 48 hours of incubation, 20 μl of MTS reagent (Promega, Madison, WI, USA) per well was added to the cell culture medium and the cells were incubated for 1 hour in the incubator. Then, the absorption was measured on microplate absorbance reader TECAN (TECANGENios, Salzburg, Austria) at a wavelength of 485 nm. Potential interference of 2DG and NP with colorimetric detection in MTS assay [28] was accounted for by using cell-free wells as a reference. Reference absorption values were subtracted from the values of the corresponding treatment wells. Data were collected by Magellan software. All analyses were performed in eight-fold.

3. Results

Using a simple one-pot preparation of water-dispersible Fe_3O_4 nanoparticles, we were able to successfully generate NPs coupled with 2-Deoxy-D-Glucose (2DG). Atom adsorption spectroscopy of the obtained samples allowed to determine that 1 g of prepared 2DG coated magnetite contains 0.418 g of 2DG.

Characterization of nanostructure

FTIR spectroscopy revealed that the spectrum of the $\text{Fe}_3\text{O}_4@2\text{DG}$ (Fig. 1) exhibited a characteristic peak of Fe_3O_4 at about 575 cm^{-1} (Fe–O stretching), the peaks at $\sim 3457.7\text{ cm}^{-1}$ are attributed to the stretching vibrations of –OH, which is assigned to –OH- absorbed by Fe_3O_4 nanoparticles. The hydrogen bond of chelate type appears as a wide degraded band in region $3500\text{--}3200\text{ cm}^{-1}$. The presence of characteristic bands in $1600\text{--}1000\text{ cm}^{-1}$ region corresponds to skeleton vibration of 2DG molecules. The pyranose ring skeletal vibrations bands are in $990\text{--}840\text{ cm}^{-1}$ region. The intensive bands in $1384\text{--}1250\text{ cm}^{-1}$ region correspond to deformation vibration of hydroxyl group. In addition, there are many well-defined peaks in the fingerprint region between 1640 and 700 cm^{-1} corresponding to 2DG. The fingerprint region of the $\text{Fe}_3\text{O}_4@2\text{DG}$ regions confirms that the 2DG molecules after adsorption on magnetite surface have not changed their structure.

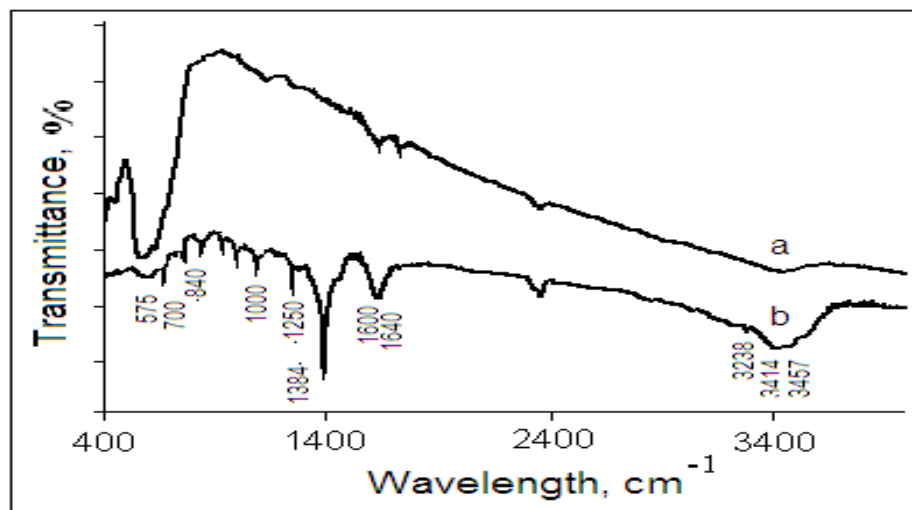


Fig. 1. FTIR spectra for the (a) pristine Fe_3O_4 , (b) $Fe_3O_4@2DG$. FTIR spectra were recorded on a Varian 3600 FTIR spectrophotometer in KBr tablets. The spectrum was taken in the range of 4000-400 cm^{-1} at room temperature. FTIR spectroscopy reveals a characteristic peak of Fe_3O_4 at about 575 cm^{-1} (Fe-O stretching)

The XRD pattern of $Fe_3O_4@2DG$ is shown in Fig.2. All the XRD peaks were well defined and correspond to Fe_3O_4 nanoparticles with spinel structure. The XRD peak broadening indicates formation of nanocrystals. In this pattern, all lines can be indexed using the ICDD no. 00-001-1111 corresponding to magnetite. The pattern has characteristic peaks at 30.36°(220), 35.68°(311), 43.3°(400), 57.36°(511), and 62.95°(440), which well correlate with the standard pattern of Fe_3O_4 . The intensity of the diffraction peak of (311) plane is stronger than the other peaks. The average crystal size estimated from this peak using the Scherrer formula is 8.5 nm.

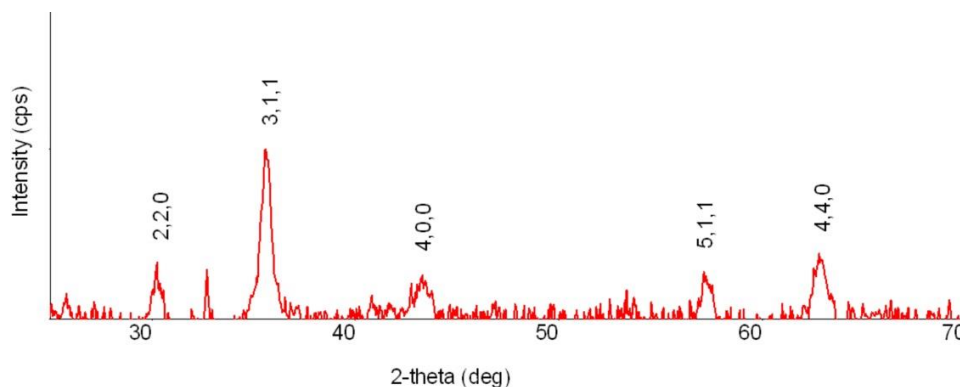


Fig. 2. XRD pattern for the nanostructured $Fe_3O_4@2DG$. A clearly defined XRD pattern was observed, corresponding to Fe_3O_4 nanoparticles with spinel structure. The average crystal size estimated from this peak using the Scherrer formula is 8.5 nm.

The morphological characteristics of the $Fe_3O_4@2DG$ composite nanoparticle determined by SEM are shown in Fig. 3(a). The composite nanoparticles were almost monodisperse with a uniform size. The coating of magnetite nanoparticles with 2DG leads to preparation of non-aggregated nanoparticles with a very narrow size distribution (approximately 6-12 nm). It proves that sizes of $Fe_3O_4@2DG$ composite nanoparticles are in a good agreement with data obtained from XRD analysis. EDS of the same samples shown in Fig.3 (b) was performed with an EDAX X-ray energy-dispersive analysis system attached to the JEOLJSM-7600F transmission electron microscope. The points identified in the EDS spectrum demonstrate the presence of Fe and O as the main elements of the sample and supports the data of magnetite nanoparticles formation (the other peaks are corresponding to Cu, C being characteristic of the carbon-coated grid).

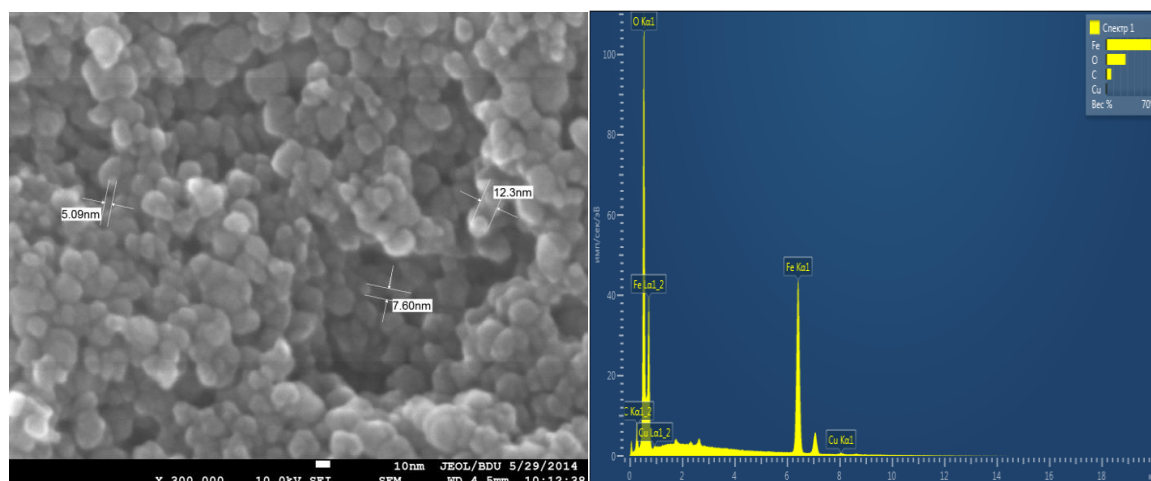


Fig. 3. (a) SEM image of $\text{Fe}_3\text{O}_4@2\text{DG}$ nanoparticles. The composite nanoparticles were almost monodisperse with a uniform size. The coating of magnetite nanoparticles with 2DG leads to preparation of non-aggregated nanoparticles with a very narrow size distribution (approximately 6-12 nm). The sizes of $\text{Fe}_3\text{O}_4@2\text{DG}$ composite nanoparticles are in a good agreement with data obtained from XRD analysis. (b) ED pattern of $\text{Fe}_3\text{O}_4@2\text{DG}$ nanoparticles. EDS was performed with an EDAX X-ray energy-dispersive analysis system attached to the JEOLJSM-7600F transmission electron microscope. The points demonstrate the presence of Fe and O as the main elements of the sample and support the data of magnetite nanoparticles formation.

The surface morphology pattern of $\text{Fe}_3\text{O}_4@2\text{DG}$ is displayed in Fig. 4. The morphology exhibits peaks caused by the magnetite nanoparticles covered by 2DG. The average sizes of formed nanoparticles were between 8-13 nm that correlates well with data obtained from XRD and SEM analysis. These results revealed that the nanoparticles were homogeneously sized and uniformly shaped.

Cell viability measurements revealed that $\text{Fe}_3\text{O}_4@2\text{DG}$ nanoparticles could reduce the number of living cells to less than 50% depending on the cell line. The effect of 2DG without nanoparticles was observed to be more pronounced than the effect of $\text{Fe}_3\text{O}_4@2\text{DG}$ at the same concentration in all three cell lines tested (Fig. 5). The reduction of viable cells after $\text{Fe}_3\text{O}_4@2\text{DG}$ treatment was significant when compared to control for all cell lines (HCT116, $p=0.004$; RKO, $p=0.002$; HT29, $p=0.001$).

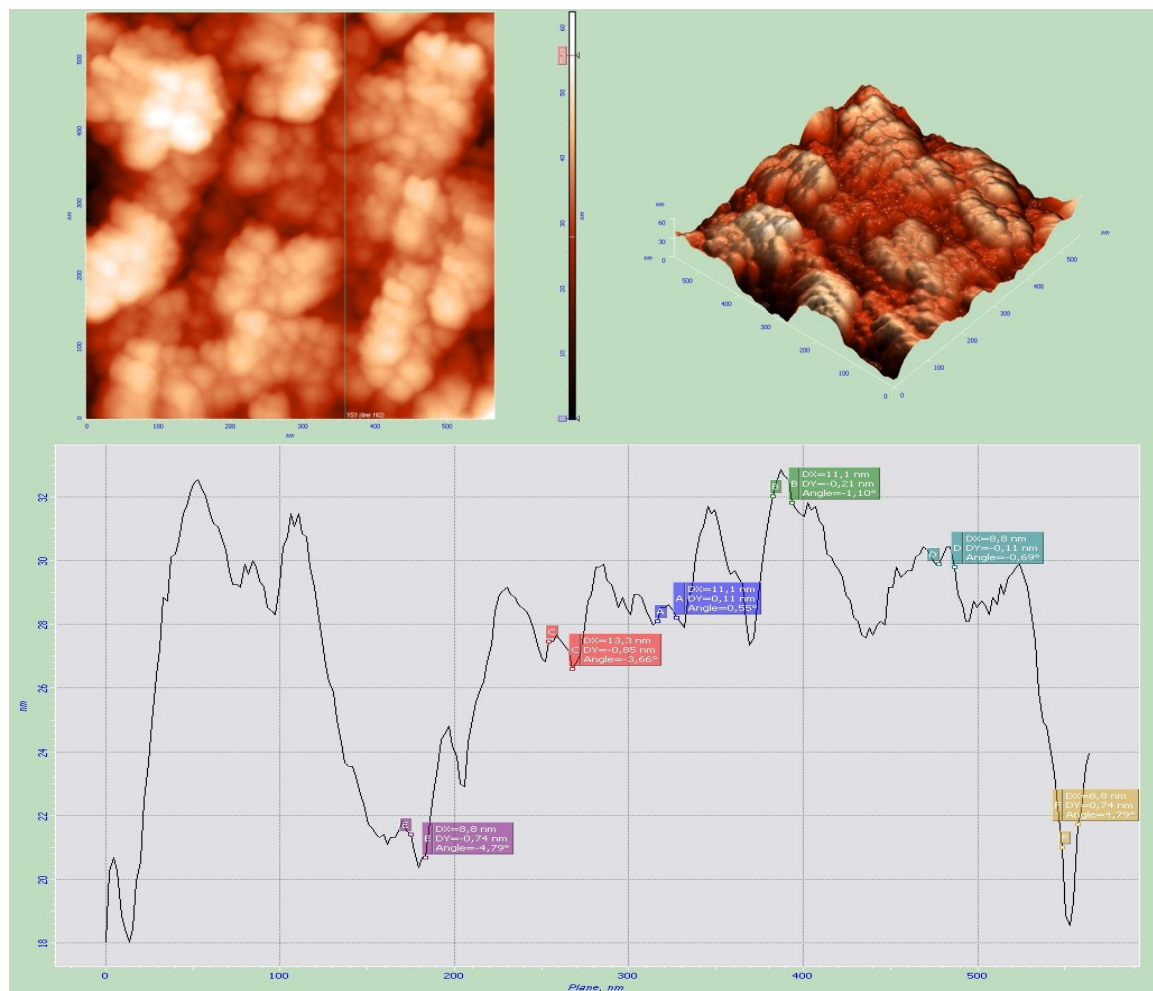


Fig. 4. AFM study of Fe₃O₄@2DG nanoparticles. (a) 2D image of Fe₃O₄@2DG NPs; (b) 3D image Fe₃O₄@2DG NPs; (c) the histogram of Fe₃O₄@2DG NP sizes. The morphology exhibits peaks caused by the magnetite nanoparticles covered by 2DG. The average sizes of formed NPs rank between 8-13 nm. The results correlate well with data obtained from XRD and SEM analysis and demonstrate that the nanoparticles are homogeneously sized and uniformly shaped.

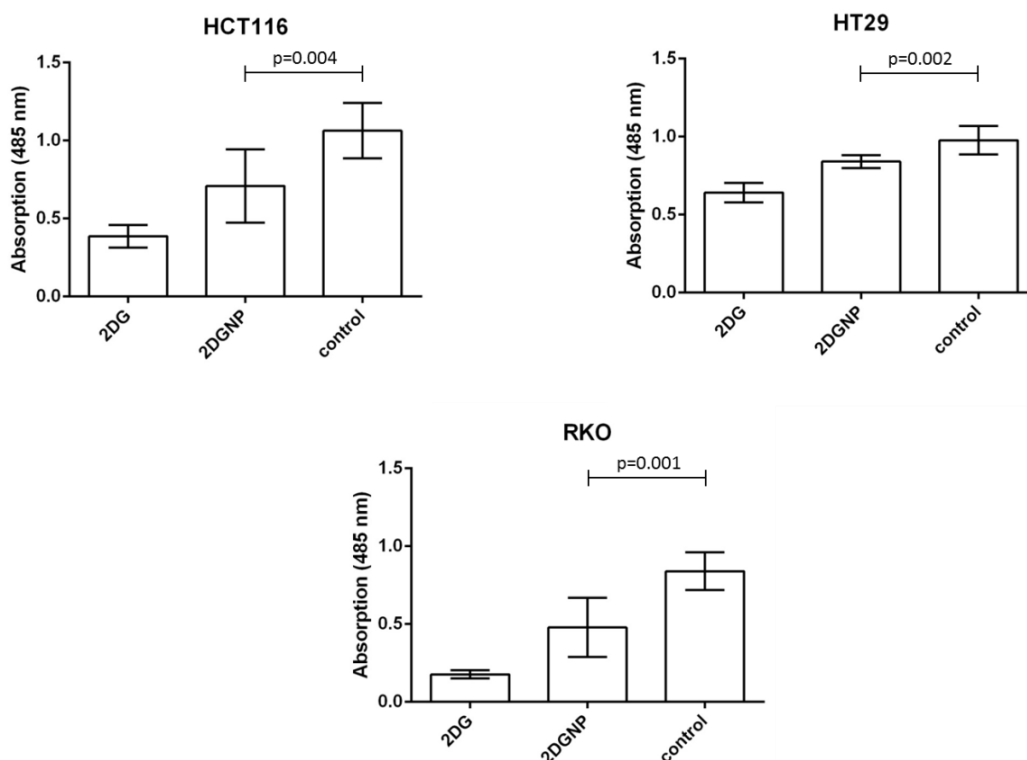


Fig. 5. Cell viability upon 2DG/ Fe_3O_4 @2DG treatment measured by MTS assay. Changes of cell viability are displayed for HCT116, RKO, and HT29 cell lines treated with 2DG or Fe_3O_4 @2DG nanoparticles for 48 hours. Y axis represents absolute absorption, error bars represent standard errors of quadruplicate measurements. A significant reduction of tumor cell viability was observed upon treatment with 2DG, but also upon treatment with Fe_3O_4 @2DG NPs compared to control for all cell lines tested.

Table 1. XRD Peak list for nanostructured Fe_3O_4 @2DG

No.	2-theta(deg)	d(ang.)	Int. I(cps deg)	Phase name	Chemical formula
1	30.3168	2.94582	763.604	Magnetite(2,2,0)	Fe_3O_4
2	35.681(17)	2.5143(11)	2424(93)	Magnetite(3,1,1)	Fe_3O_4
3	43.31(6)	2.088(3)	990(83)	Magnetite(4,0,0)	Fe_3O_4
4	57.363	1.60498	653.404	Magnetite(5,1,1)	Fe_3O_4
5	62.95(4)	1.4753(8)	1060(103)	Magnetite(4,4,0)	Fe_3O_4

4. Discussion

A new water-dispersible nanostructure based on SPIONs (Fe_3O_4) coated by 2DG was prepared in a well-shaped spherical form by chemical co-precipitation. The prepared nanoparticles were found to be well individualized and homogeneous with narrow size distribution of approximately 6-12 nm.

2DG has various properties that make it an ideal candidate for coupling to NPs. The carbohydrate molecules within 2DG can stabilize and functionalize the surface of iron oxide NPs [29-32]. Moreover, the 2DG hydroxyl groups enable chelation and hydrogen bonding with iron oxide surfaces. Coordination of 2DG molecules as ligands on the surface of Fe_3O_4 NPs occurs due to self-assembly of carbohydrate molecules by non-covalent interaction, which allows simple

synthesis without requiring additional stabilizer molecules. At the same time, 2DG creates a physical barrier, which prevents spontaneous agglomeration. In comparison with polymeric ligands, 2DG has a small size, which gives the particles a small hydrodynamic radius. A small hydrodynamic radius is preferable for efficient biomedical application in vivo [33,34]. In addition, anti-tumoral efficacy of 2DG shown in numerous studies makes it particularly interesting candidate for coupling with NPs for its possible further medical application.

The newly established particles may be applicable in various clinical and non-clinical settings. For example, 2DG coupled NPs may possibly be used to specifically target glucose-dependent cancer cells sparing at the same time normal tissues using the ability of SPIO NPs to deliver the coupled drug to the site of interest. Moreover, synthesized NPs might be applied also in the diagnostic setting, where the sensitive properties for tumor detection based on the principle used in PET might be combined with alternative visualization tools for the detection of magnetic particles.

To provide first proof-of-principle that the growth-inhibitory effects of 2DG on tumor cells are in fact maintained after coupling to magnetic SPIO NP, we selected three colorectal cancer cell lines with variable, but significant sensitivity to 2DG. To ensure comparability of the Fe₃O₄@2DG effects with 2DG alone, we determined 2DG concentration in Fe₃O₄@2DG preparations and adjusted concentrations accordingly. Cell viability analysis revealed that at equivalent concentrations, the effect of 2DG alone was higher than the effect of Fe₃O₄@2DG. This may be caused by physical and chemical reasons like 2DG release kinetics or direct interaction of nanoparticles with cellular receptor or transporter molecules that are unknown so far.

In summary, we here show successful coupling of 2DG to SPIO NPs, maintaining the structural and functional properties of 2DG. Using a broad spectrum of physicochemical analyses, we demonstrate that the newly established Fe₃O₄@2DG NPs possess a uniform size within a narrow size range. Fe₃O₄@2DG NPs may become a promising tool for targeted drug delivery. Though it has to be conceded that the potential superiority of Fe₃O₄@2DG compared to 2DG in a medical context can only be proven in suitable preclinical models, our data demonstrate that 2DG maintains its anti-tumoral activity even after coupling to NP.

References

- [1] J. Behary J. of experimental biology **48**, 1008 (2010).
- [2] P. Tartaj, M. P. Morales, T. Gonzalez-Carreno, S.V-Verdaguer and C. J. Serna, J. Magn. Magn. Mater. **290**, 28 (2005).
- [3] A.M.Maharramov, I.N. Alieva, G.D.Abbasova, M. A. Ramazanov, N.S.Nabiyev, M. R. Saboktakin DJNB, **2**, 463 (2011).
- [4] Mohammad Reza Saboktakin , Abel Maharramov, Mohammad Ali Ramazanov Journal of Non-Oxide Glasses **1**(3), 211 (2009).
- [5] Nguyen T.K. Thanha; Luke A.W. Green Nano Today **5**, 213 (2010).
- [6] S Rajesh Kumar; Lucafo Marianna; Sava Gianni; A Joseph Nathanael; S I Hong; Tae Hwan Oh; D Mangalaraj; C Viswanathan and N Ponpandian J.Materials Research Express **1** (2014)
- [7] J. Giri, S.G. Thakurta, J. Bellare, A.K. Nigam, D. Bahadur, J. Magn. Magn. Mater. **293**, 62 (2005).
- [8] M.D. Senarath-Yapa, S. Phimpivong, J.W. Coym, M.J. Wirth, C.A. Aspinwall, S.S. Saavedra, Langmuir **23**, 12624 (2007).
- [9] Abel Maharramov, Mahammadali Ramazanov, Mohammad Reza Saboktakin Advanced Nanocomposites Types, Properties, and Applications Nova Publisher, Nyu York, 2013, 334 p.
- [10] A.G. Kanaras, Z.X. Wang, A.D. Bates, R. Cosstick, M. Brust, Angew. Chem. Int. Ed. **42**, 191 (2003).
- [11] M. Cardenas, J. Barauskas, K. Schillen, J.L. Brennan, M. Brust, T. Nylander, Langmuir **22**, 3294 (2006).
- [12] R. Mahtab, H.H. Harden, C.J. Murphy, J. Am. Chem. Soc. **122**, 14 (2000).
- [13] S. Pathak, S.K. Choi, N. Arnheim, M.E. Thompson, J. Am. Chem. Soc. **123**, 4103 (2001).

- [14] S. Chairam, E. Somsook, J. Magn. Magn. Mater. **320**, 2039 (2008).
- [15] S. Chairam, C. Poolperm, E. Somsook, Carbohydr. Polym. **75**, 694 (2009).
- [16] K.C. Ho, P.J. Tsai, Y.S. Lin, Y.C. Chen, Anal. Chem. **76**, 7162 (2004).
- [17] K. Nishimura, M. Hasegawa, Y. Ogura, T. Nishi, K. Kataoka, H. Handa, et al., J. Appl. Phys. **91**, 8555 (2002).
- [18] M. Lewin, N. Carlesso, C.H. Tung, X.W. Tang, D. Cory, D.T. Scadden, et al., Nat. Biotechnol. **18**, 410 (2000).
- [19] R. Levy, N.T.K. Thanh, R.C. Doty, I. Hussain, R.J. Nichols, D.J. Schiffrin, et al., J. Am. Chem. Soc. **126**, 10076 (2004).
- [20] C. Sun, J.S.H. Lee, M.Q. Zhang, Adv. Drug Deliv. Rev. **60**, 1252 (2008).
- [21] S. Laurent, D. Forge, M. Port, A. Roch, C. Robic, L.V. Elst, et al., Chem. Rev. **108**, 2064 (2008).
- [22] K. Cheng, S. Peng, C.J. Xu, S.H. Sun, J. Am. Chem. Soc. **131**, 10637 (2009).
- [23] D.W. Inglis, R. Riehn, R.H. Austin, J.C. Sturm, Appl. Phys. Lett. **85**, 5093 (2004).
- [24] A. Jordan, R. Scholz, P. Wust, H. Fahling, R. Felix, J. Magn. Magn. Mater. **201**, 413 (1999).
- [25] D.S. Wen, Int. J. Hyperthermia **25**, 533 (2009).
- [26] Haibin Xi, Metin Kurtoglu, Theodore J. Lampidis VC 2014 IUBMB V. **66**(2), 110 (2014).
- [27] B Dwarakanath, D Singh , A Banerji, R Sarin, N Venkataramana, R Jalali, P Vishwanath, B Mohanti, R Tripathi, V Kalia, V. Jain, J Cancer Res Ther. 798 (2009).
- [28] AL Holder, R Goth-Goldstein, D Lucas, CP. Koshland j. Chem Res Toxicol. 1885 (2012)
- [29] S. Laurent; C. Nicotra; Y. Gossuin, A. Roch; A. Ouakssim, Elst, L. Vander, M. Cornant, P. Soleil, R. N. Muller, Phys. Status Solidi, **12**, 3644 (2004).
- [30] L. F. Gamarra, G. E. S. Brito; W. M. Pontuschka, E. Amaro, A. H. C. Parma, G. F. J. Goya, Magn. Magn. Mater., **289**, 439 (2005).
- [31] R. S. Molday, D. MacKenzie J. Immunol. Methods, **52**, 353 (1982).
- [32] K. G. Paul, T. B. Frigo, J. Y. Groman, E. V. Groman, BioconjugateChem. **15**, 394 (2004).
- [33] F.R. Li, W.H. Yan, Y.H. Guo, H. Qi, H.X. Zhou, Int. J. Hyperthermia 25, 383 (2009)—391
- [34] M. Longmire, P.L. Choyke, H. Kobayashi, Nanomedicine **3**, 703(2008).
- [35] Massart R (1981). IEEE , 1247